2011-10-10

Preparation and Characterization of a Composite of Gold Nanoparticles and Single-Walled Carbon Nanotubes and Its Potential for Heterogeneous Catalysis

Anne Shanahan
Technological University Dublin, Anne.Shanahan@tudublin.ie

James Sullivan
University College Dublin, james.sullivan@ucd.ie

Mary McNamara
Technological University Dublin, Mary.McNamara@tudublin.ie

See next page for additional authors

Recommended Citation

Shanahan, A. et al (2011) Preparation and Characterization of a Composite of Gold Nanoparticles and Single-Walled Carbon Nanotubes and Its Potential for Heterogeneous Catalysis. *New Carbon Materials,* Vol.26, 5, p.347-355. doi:10.1016/S1872-5805(11)60087-560087-5

Funder: INSPIRE,DIT

Preparation and characterisation of a Gold Nano-particle Single Walled Carbon Nanotubes composite and preliminary study of its heterogeneous catalytic potential.

Anne E Shanahan [ab,*], James A Sullivan [c], Mary McNamara [a], Hugh J Byrne [b]

[a] School of Chemical and Pharmaceutical Sciences, Dublin Institute of Technology, Kevin St, Dublin 8, Republic of Ireland.

[b] FOCAS Research Institute, Dublin Institute of Technology, Camden Row Dublin 8, Republic of Ireland.

[c] UCD School of Chemistry and Chemical Biology, Belfield, Dublin 4, Republic of Ireland.

Abstract

A single walled carbon nanotube supported gold composite was prepared and this composite was characterized by XRD, STEM/SEM/TEM, EDX, AAS, BET, Raman spectroscopy and UV-Visible spectroscopy. The particles were found to be crystalline and have a well defined and narrow particle size distribution centred on 7nm. The activity and selectivity of the composite for solventless aerobic oxidation of a secondary alcohol was examined and conversion efficiencies of 95% were found.

Keywords: SWCNT, gold nanoparticle composite, catalysis

* Corresponding author. Tel: +353-1-4027905

Fax: +353-1-4027904

Email: anne.shanahan@dit.ie

Author introduction: Anne E Shanahan (1975-), female, Technical Support for the Focas Research Institute which is the multi disciplinary science based research facility for Dublin Institute of Technology. Areas of expertise lie in advanced analytical chemistry, carbon nanotubes and more recently in heterogeneous catalysis. Tel: +353-(0) 1-4027905, Fax: +353-(0) 1-4027904, E-mail: anne.shanahan@dit.ie

1. Introduction

Carbon nanotubes have attracted significant interest as the basis for applications to new materials and device concepts in areas such as nanoelectronics and solar cells due to their unique structural, mechanical and electronic properties [1, 2]. For example, both single walled and multi walled carbon nanotubes have been proposed as substrates for biological devices [3]. Metal filled carbon nanotubes have also been shown to have promising applications in heterogeneous catalysis [4] and multi walled carbon nanotubes have been used as catalyst supports in thermal and electro catalysis [5,6]. In addition, MWCNTs have been successfully used as supports for electrocatalysts [7] and gold nanoparticles supported on SWCNT films have already been shown to be promising electrochemical sensors [8].

However as is now widely known by researchers in the area, SWCNT are notoriously difficult to solubilise which would generally render conventional methods of composite preparation useless. Conversely Dai, *et al* have demonstrated a directed reduction route of Au^{3+} onto the sidewalls of SWCNT without requiring further chemical processing [9]. The downside to this method however is the broad diameter distribution of the gold nanoparticles. By streamlining this method, it is possible to produce Au nanoparticles with a narrow particle distribution. SWCNT as a support, provide a template of narrow diameter distribution fibres which allow the constrained growth of metal nano-particles to a narrow diameter range.

As aforementioned, several applications across the scientific disciplines have been considered for carbon nanotubes including catalysis [10, 11] and in this work preliminary catalytic testing of the Au/SWCNT composite material for use in green chemical reactions owing to the catalytic activity of nanoparticulate (d_{Au} = 1-10nm) gold has been carried out. Au catalysts have been an area of intense research activity in recent times [12-17]. One area in particular where such catalysts have found application is in environmentally friendly oxidation reactions, *e.g.* in the selective oxidation of CO from H_2-containing streams [18, 19] and in selective oxidations using O_2 as an oxidant [20-26].

In general, oxidation reactions play an important role in the synthesis of pharmaceuticals, bulk and fine chemicals. However, classical oxidation reactions generally involve the use of chemicals and reaction systems that are not environmentally friendly, (*e.g.* permanganate and other acidified transition metal systems) [27, 28]. The reagents and waste products produced can be toxic and difficult to remove from process streams and are thus undesirable. A "greener" alternative to such processes is aerobic oxidation using a heterogeneous catalyst. This option is preferred as O_2 is inexpensive, non-toxic and produces water as the sole by-product. However, commonly employed catalyst systems are often prepared/operate at high temperatures requiring significant modifications to the synthetic design. Nanoparticulate materials are an alternative to such conventional catalysts. However, their characteristics and activity can further depend on their support substrate. Haruta has demonstrated for example that the catalytic properties of gold are dependent on both the particle size and the support [29].

Au particles of diameter range ~7.5 nm – 350 nm supported on carbon have been investigated previously in the oxidation of glycerol [30] and the system was shown to be selective for the formation of glyceric acid. Prati, *et al* [31] were able to improve this selectivity (defined in this case as the ability of the catalyst to promote the formation of a particular compound from a reaction when several products are feasible) considerably by optimizing both the catalyst preparation method and the reaction conditions. Most notable however is that the principle developments were based on control of particle size.

A further area in which supported gold catalysts have been used is in environmentally friendly oxidations such as the liquid-phase oxidation of 1-Phenylethanol to Acetophenone. Notably, nano Au has been reported to have superior performance to nano Pd in this reaction [32]. Nano Au supported on mixed metal oxides has also been tested in this liquid-phase oxidation by Baiker, *et al* [33] and the system has been shown to be somewhat suitable for this type of reaction but the performance appears to be very dependent on Au particle size which in turn is critically dependent on the support mechanism.

The ability to control the size and diameter range therefore has potential to provide routes towards optimisation of the catalytic process.

In this work, the growth and characterisation of Au nanoparticles supported on SWCNT templates is reported. They are thoroughly characterised using a number of microscopic, structural and spectroscopic techniques and their potential suitability as catalysts for "green reactions" is demonstrated using the Au catalysed aerobic oxidation of 1-phenylethanol, we believe for the first time.

2 Experimental

2.1 Composite preparation

Hydrogen tetrachloroaurate (III) trihydrate $HAuCl_4.3H_2O$ (>99%), Arc-Discharge Single Walled Carbon Nanotubes [SWCNT] (~70% SWCNT, ~30% Carbon, <1% Nickel/Yttrium, average radius of 1.4nm) and Sodium Borohydride ($NaBH_4$) were purchased from Sigma-Aldrich. All materials were used without further purification.

Gold supported on SWCNT (5%wt) catalyst was prepared via an *in-situ* reduction method similar to that reported by Scurrell *et al* [34] for the preparation of TiO_2 supported nanoparticulate catalysts. In summary, this involves the reduction of an Au (III) salt to Au (0) onto the sidewalls of the SWNT.

2.2 Composite characterisation

The composite and precursor support were characterised by powder X-Ray diffraction using a Phillips diffractometer with a monochromatic Cu $K\alpha_1$ source operated at 40keV and 30mA.

The surface area of the prepared composite and SWCNT support were determined by multi point N_2 adsorption using a Gemini VI 2000e Surface Area Analyser at 77K and data analysis was carried out using the Brunauer Emmett Teller (BET) method from the N_2 adsorption isotherms.

Energy Dispersive X-Ray Analysis (EDX) was carried out using a Jeol 8600 microprobe. This microprobe consists of an electron gun and a series of electromagnetic lenses for collimating the beam. In addition it contains scanning coils to allow the beam to be rastered across the specimen. For sample analysis, the composite samples were scattered onto a Silver DAG conductive paint on a copper sample stub.

Atomic Absorption Spectroscopy (AAS) (Varian Spectr200), with a calibration plot was used to determine the Au loading following acid digestion of the composite.

Scanning Transmission Electron Microscopy (STEM) and Scanning Electron Microscopy (SEM) imaging were carried out using a Hitachi SU6600 variable pressure field emission SEM with a Schottky field emission electron gun which provides in excess of 200 nA probe current. Samples of the composite and the precursor support were prepared for STEM following dispersion in ethanol. A drop of the suspension was then placed on a holey carbon film supported on a 300 mesh copper TEM grid. Samples for SEM were prepared by stabilising the powders on carbon tab. The size distribution of the Au nanoparticles was evaluated using AxioVision LE software (Carl Zeiss).

Transmission Electron Microscopy (TEM) imaging was also accomplished using a JEOL JEL-2000 EX electron microscope with a lattice resolution of 0.14nm and a point-to-point resolution of 0.3nm operating at 80 kV. Samples for TEM were prepared in exactly the same manner as those for STEM.

Raman Spectroscopic analysis was carried out using a Horiba Jobin Yvon LabRAM HR 800. Light is imaged to a diffraction limited spot (typically 1 micron) via the objective of an Olympus BX50 microscope. The scattered light is collected by the objective in a confocal geometry, and is dispersed onto an air cooled CCD array by one of two interchangeable gratings, 300 lines/mm or 600lines/mm, allowing the range from 150cm^{-1} to 4000cm^{-1} to be covered in a single image, or with greater resolution in a combination of images. For Raman analysis, the SWCNT precursor support and the Au/SWCNT composite were placed on a microscope slide. Measurements were carried out using a 660nm solid state diode laser (100mW) standard bandwidth version with double edge filter upgrade (cut off to 70cm^{-1}).

UV-Vis spectroscopy was carried out using a Perkin Elmer Lambda 900 UV/VIS/NIR spectrometer which is a double-beam, double monochromator ratio recording system with pre-aligned tungsten-halogen and deuterium lamps as sources. The wavelength range is from 175 to 3300nm with an accuracy of 0.08 nm in the UV-Visible region and 0.3nm in the NIR region guaranteed. It has a photometric range of +/-6 in absorbance mode. Samples for UV-Vis were prepared by dispersing SWCNTs or Au/SWCNT composites (0.4 mg) in 15 ml of deionised water and sonicating for 60 seconds using a sonic tip (ultrasonic processor VCX, 750W) prior to analysis.

.

2.3 Oxidation experiments

The oxidation reactions were carried out at atmospheric pressure by solventless aerobic oxidation of 1-phenylethanol using a Dean-Stark trap to collect the water formed under the following reaction conditions: T = 120ºC, 207mmol of substrate (substrate to catalyst mass ratio 1 : 0.002) and O_2 flow rate of 35 mL min^{-1} for 3h.

Liquid phase oxidation products were monitored using FTIR spectroscopy and HPLC analysis and then confirmed using ^{1}H and ^{13}C NMR spectroscopy. Scheme 1 shows the reaction of interest.

3. Results and Discussion

3.1 Material Characterisations

EDX analysis of the Au/SWCNT composite was carried out and clearly showed the presence of gold with signals at both 2keV (M line) and 10keV (L Line).

The EDX results were confirmed by AAS of the acid extracted samples which showed a gold loading of 5.2% for the Au/SWNT composite material

Specific surface areas and textural characteristics are determined by the BET/BJH methods. Both the supports and the Au loaded samples show characteristic Type IV adsorption isotherms (IUPAC classification) which indicate that they have mesoporous regions (shown in Figures 1A and B). Adsorption of N_2 at low pressures confirms that both have micro-porosity also [35]. The specific surface area increases when Au is deposited onto the supports, as expected for a relatively small

loading of particles on a fibre mesh. The specific surface area of the SWCNT support was determined to be 249 m^2g^{-1} whereas for the Au/SWCNT it is 265 m^2g^{-1}.

The meso and microporosity of the SWCNT supported sample is relatively unchanged following the deposition. The average pore diameters for both the mesoporous and microporous regions were calculated taking into account the shape of both the adsorption and desorption branches of the isotherm as well as the hysteresis loops using the BJH method based on the Kelvin Equation [36]. For Au/SWCNT d_{mes}= 6.3 nm and d_{mic}= ~0.8 nm. In contrast the untreated SWCNT had d_{mes}= 6.1 nm and d_{mic}= ~0.7 nm.

The crystallinity of the composite and support was shown through analysis of their XRD patterns. The diffractograms, shown in Figure 2, confirm the crystalline phases present in the materials. The XRD profile of the support shows reflections at 2θ= ~45º [corresponding to CNT (004) and 2θ = ~ 52º corresponding to Ni (200)]. There is a broad feature centred at 2θ = ~23º. The XRD of the composite material shows peaks at 2θ= ~38.5º, ~45.2º and 65.2º which correspond to Au (111), (200) and (311) reflections indicating the formation of Au nanoparticles with a face centred cubic structure [37].

The sizes of the gold particles on the composite were estimated using the Scherrer equation (which assumes the particles are spherical) [38] applied to the Au (111) reflection at 38.5º. It was found that the Au nanoparticles on SWCNT have an average particle size of 4.7nm.

The morphologies of the Au/SWCNT composite were investigated using STEM. The average Au particle size (n=100) was also calculated using this technique.

Figures 3A and B show representative samples of the STEM images obtained from the Au/SWCNT composite. Figure 3A, using a magnification of x30,000, gives an overall indication of the morphology of the composite. The SWCNT are well dispersed and although not fully exfoliated, are present in bundles of diameter significantly less than the rope like structures of the as produced samples, which are several microns in length and have bundles of diameter ~30nm (shown in Figure 4A). It can be seen that the Au nanoparticles are reasonably homogeneously dispersed [Figure 3A] and appear to be adhered on the SWCNT surfaces. Figure 3B shows two of the SWCNT structures and shows the Au particles sitting on the backbone of the SWCNT. The accelerating voltage was reduced to minimise deposition of in beam contamination onto the sample during imaging at higher magnifications as well as charging effects. The image shows two of the SWCNT structures and both individual Au nanoparticles as well as agglomerates of mostly amorphous carbon sitting on the backbone of the SWCNT.

In addition, a small proportion of the Au particles on the SWCNT do not appear to be well defined in shape. The particle size distribution was estimated using AxioVision LE's integrated camera controls. After that the program's interactive histogram and image processing tools allowed optimization of the colour, contrast and brightness of the image as well as image analysis and measurement functions. Although there are some Au aggregates visible, the particle size distribution is sharply peaked and the average particle size is estimated to be ~7nm for Au/SWCNT which is in good agreement with the value calculated from the XRD data, assuming spherical particles.

Figure 4A shows a higher magnification SEM image of the morphology of the partially debundled SWCNT with the large particles attributed to amorphous carbon. Figure 4B shows stabilised Au nanoparticles and thus the narrow diameter range achievable and finally Figure 4C shows the Au/SWCNT composite in which the atomic weight (z) ratios (determined by the greyscale of the image) show a clear difference between the amorphous carbon impurities and the gold nanoparticles present on the SWCNT backbones as well as the change in the bundle sizes of the tubes themselves.

Raman Spectroscopy has been extensively used to probe the properties of single walled carbon nanotubes [39, 40]. Figure 5 shows the Raman spectra of raw SWCNT and the Au/SWCNT composite. In general, SWCNT display four clear areas of interest in a Raman spectrum. The Radial Breathing Modes (RBM) in the low frequency region (~100 - 400cm^{-1}) are associated with the vibration of carbon atoms in a radial direction in relation to the carbon nanotube axis and are often used to calculate the diameter of isolated SWCNT. The RBM's are exclusive to SWCNT and are in themselves proof of the presence of SWCNT in a sample.

The tangential mode (D and G) incorporates three modes, D at ~ 1300cm^{-1}, G^+ at ~1590cm^{-1} and G^- at ~1570cm^{-1}. D is a phonon mode disorder band that is accepted to be due to defects that break the symmetry of the graphene plane in the sample and tends to increase in intensity with doping [39, 40]. G^+ is associated with carbon atom vibrations along the nanotubes axis. G^- is associated with vibrations of the carbon atoms along the circumferential direction.

The G band frequency and shape is also used to distinguish between semiconducting and metallic SWCNTs. Finally the G' band at ~2700 cm^{-1} is an overtone of the D band. The peaks at ~580 cm^{-1} and ~1100 cm^{-1} are contributions from the underlying microscope slide.

There are several differences between the spectra shown in Figure 3. The G^+ band has shifted upfield from 1591 cm^{-1} to 1597 cm^{-1} in the composite sample which is indicative of charge transfer onto the SWCNT [41]. This suggests that the Au nanoparticles have lost electrons to the SWCNT and in the process have become positively charged. In contrast, the G^- band at 1577 cm^{-1} has become more prominent in the composite sample. This suggests the presence of nanotubes of metallic character in the sample. Finally the G' band at 2668 cm^{-1} has become more pronounced and has red-shifted in the composite and the D band at ~1337 cm^{-1} has upshifted to ~1343 cm^{-1} These types of changes have been attributed to the presence of metallicity either from doping or preferential selection of the metallic SWCNT interacting with the Au nanoparticles [42].

The UV-Visible absorption spectra of SWCNT and Au/SWCNT are shown in Figure 6. Both spectra show the characteristic π plasmon band of SWNTs at ~270 nm [43]. The SWCNT spectrum shows very weak bands at ~700 nm and 750 nm that correspond to the electronic transitions between the Van Hove singularities in the nanotube density of states, in these cases the E_{11} transitions for metallic arc discharge nanotubes [44] (see inset). The Au/SWCNT shows an additional clear broad absorption band at ~560 nm which corresponds to a Au surface plasmon resonance band [44] and is characteristic of suspended Au particle sizes of ≤15nm [45]. In the spectrum of the composite material, the π plasmon band is somewhat dampened and red shifted by the presence of the Au nanoparticles. The observed decrease of peak intensity at 270 nm in the raw SWCNTs compared to the composite sample in addition to a red shift in this band of ~8 nm in the Au/SWCNT composite spectrum both suggest that the π-π interactions between the SWCNT and the Au [46] contribute to the binding between the Au nanoparticles and the SWCNT surfaces. The spectra of the aqueous dispersions thus indicate that the nano particles remain adhered to the SWCNT template.

3.2 Catalytic Activity Measurements

During the oxidation reactions, acetophenone and water were the only products formed. The reactions were carried out in triplicate using fresh catalyst to ensure reproducibility. The Au/SWCNT catalyst gave a reactant conversion of 95% after 180min.

Figure 7 shows the conversion of 1-phenylethanol into acetophenone using O_2 over an Au/SWCNT catalyst as a function of time. The error bars indicate the variation over three independent reactions illustrating the reproducibility of the reaction.

Recent work on catalytic selective oxidation of 1-phenylethanol amongst other alcohols using nano Au supported on mixed Ga/Al oxides [47] gave a comparable conversion but required the use of a solvent whereas it has been demonstrated here that Au nanoparticles supported on SWCNT yields a conversion of ~95% in a solventless system which adheres more closely to principles of green chemistry [48] which demonstrates that using SWCNT as a support material for heterogeneous catalytic functions provides some further expansion in the area of carbon nanotube chemistry.

In addition, the methodology utilized in this work thus produces not only high purity, crystalline Au nanoparticles of diameters with a majority of <10nm, but also a narrow diameter distribution which is constrained by the well defined diameter distribution of the SWCNT nano template.

4 Conclusions

A 5% Au/SWCNT composite material has been synthesised and thoroughly characterised using N_2 physisorption, UV-Visible and Raman spectroscopies, XRD, EDX, AAS and STEM. In the process of the composite preparation, the nanotubes are partially exfoliated compared to their as produced state and present a fibrous mesh of uniform diameter as support for nanoparticle growth. The Au nanoparticles (with average sizes ranging from ~6 to 8nm) as measured by STEM and XRD) adhere to the SWCNT surface and there appears to be an electronic interaction between the nanoparticles and the SWCNT involving transfer from the Au nanoparticles to the SWCNT. The diameter distribution is sharply peaked as a result of the uniformity of the support template.

The 5% Au/SWCNT composite has been demonstrated to be an active and selective catalyst for the solvent free liquid phase selective aerobic oxidation of 1-phenylethanol to acetophenone.

Acknowledgements and Dedication

The SEM and Raman instruments were purchased under the framework of the INSPIRE programme, funded by the Irish Government's Programme for Research in Third Level Institutions, Cycle 4, National Development Plan 2007-2013, supported by the European Union Structural Fund.

AES would like to thank the Focas Research Institute at the Dublin Institute of Technology for the financial assistance to make this work possible and also Petrica Dulgheru at University College Dublin for the TEM imaging work.

This work is dedicated to the late Mary Mulvey

References

[1] Mintmire J W, White C T. Electronic and structural properties of carbon nanotubes. Carbon, 1995, 33, 7, 893-902

[2] Salvetat J P, Bonard J M, Thomson N H. Mechanical properties of carbon nanotubes. Applied Physics A: Materials Science and Processing, 1999, 69, 3, 255-260

[3] Ramanathan T, Fisher F T, Ruoff R S, et al. Amino-functionalised carbon nanotubes for binding to polymers and biological systems. Chem. Mater, 2005 17 (6), 1290–1295

[4] Planeix J M, Coustel N, Coq B, et al. Application of carbon nanotubes as supports in heterogeneous catalysis .J. Am. Chem. Soc. 1994, 116 (17), 7935–7936

[5] Styers-Barnett D J, Ellison S P, Park C, et al. Ultrafast dynamics of single walled carbon nanotubes dispersed in polymer films. J. Phys. Chem. A, 2005, 109 (2) 2005 289-292

[6] Auvray S, Derycke V, Goffman M, et al. Chemical optimization of self-assembled carbon nanotube transistors. Nano Letters, 2005, 5(3) 451-455

[7] Santhosh P, Gopalan P, Lee A. Gold nanoparticles dispersed polyaniline grafted multiwall carbon nanotubes as newer electrocatalysts: Preparation and performance for methanol oxidation. J Catal. 2006, 238(1), 177-185

[8] Kong J, Chapline M G, Dai H J. Functionalised carbon nanotubes for molecular hydrogen sensors. Adv Materials, 2001, 13(18) 1384-1386

[9] Dai H, Choi H C, Shim M, et al. Spontaneous reduction of metal ions on the sidewalls of carbon nanotubes. J. Am. Chem. Soc, 2002, 124, 9058-9059

[10] Cassell A M, Ng H T, Delzeit L, et al. High throughput methodology for carbon nanomaterials discovery and optimization. Applied Catalysis A, 2003 254 (1), 85-96

[11] Che G, Lakshmi B B, Martin C R, et al. Metal-nanocluster-filled nanotubes: catalytic properties and possible applications in electrochemical energy storage and production. Langmuir, 1999 15(3), 750-758

[12] Bond G C. Gold: a relatively new catalyst. Catal Today, 2002, 72, 5-9

[13] Haruta M and Date M. Advances in the catalysis of Au nanoparticles. Appl Catal, 2001, 222, 427-437

[14] Bond G C and Thompson D T. Catalysis by gold. Cat Rev – Sci Eng, 1999, 41, 319-388

[15] Mizuno N, Misono M. Heterogeneous catalysis. Chem. Rev, 1998, 98(1), 199–218

[16] Hutchings G J and Haruta M. A golden age of catalysis: a perspective. Appl Catal A, 2005, 291, 2-5

[17] Corti C W, Holliday R J, Thompson D T. Commercial aspects of gold catalysts. Appl Catal A, 2005, 291, 253-261

[18] Duck Park E, Lee D, Lee H C. Recent progress in selective CO removal in a H2-rich stream Catal Today, 2009, 139, 280-290

[19] Solsona B, Garcia T, Jones C, et al. Supported gold catalysts for the total oxidation of alkanes and carbon monoxide. Applied Catalysis A, 2006, 312, 67-76

[20] Turner M, Golovko V B, Owain P, et al. Selective oxidation with dioxygen by gold nanoparticle catalysts derived from 55-atom clusters. Nature, 2008, 454, 981-983

[21] Oxidation of alcohols and sugars using Au/C catalysts: Part 1. Alcohols. Applied Catalysis A: General, 2005, 291, 199-203

[22] Su D S, Maksimoma N, Delgado J J, et al. Nanocarbons in selective oxidative dehydrogenation reaction. Catal Today, 2005 102-103, 110-114

[23] Beilla S , Castiglioni G L , Fumagalli C, et al. Applications of gold catalysts to selective liquid phase oxidation. Catal Today, 2002, 72, 43-49

[24] Haruta M. Catalysis: Gold rush. Nature, 2005, 437(7092), 1098-99

[25] Tembe S T, Patrick G, Scurrell M S, Acetic acid production by selective oxidation of ethanol using Au catalysts supported on various metal oxide. Gold Bulletin, 2009, 42(4), 321-327

[26] Villa A, Veith G M, Prati L. Selective oxidation of glycerol under acidic conditions. Angewandte Chemie, 2010, 49, 26, 4499-4502

[27] Shaabani A, Rad F T, Lee D G. Potassium permanganate oxidation of organic compounds. Synthetic Communications, 2005, 35, 571-580

[28] Goldshleger N F. Fullerenes and fullerene-based materials in catalysis. Fullerene Science and Technology, 2001, 9(3), 255-280

[29] Haruta M. Size and support-dependency in the catalysis of gold. Catal Today, 1997, 36, 153-166

[30] Demirel S, Lehnert K, Lucas M, et al. Use of renewables for the production of chemicals : Glycerol oxidation over carbon supported gold. Applied Catalysis B:Environmental, 2007,70, 637-643

[31] Porti F, Prati L. Selective oxidation of glycerol to sodium glycerate with gold-on-carbon catalyst: an insight into reaction selectivity. J. Catal, 2004 224, 397-403

[32] Abad A, Almela C, Corma A, et al. Efficient chemoselective alcohol oxidation using oxygen as oxidant: Superior performance of gold over palladium catalysts. Tetrahedron, 2006 62, 6666-6672

[33] Haider P, Grunwaldt J D, Baiker A. Gold supported on Mg, Al and Cu containing mixed oxides: Relation between surface properties and behaviour in catalytic aerobic oxidation of 1-phenylethanol. Catalysis Today, 2009, 141, 349-354

[34] Mallick K, Witcomb M, Scurrell M. Supported gold catalysts prepared by in situ reduction technique: preparation, characterisation and catalytic activity measurements. Applied Catalysis A: General, 2004, 259, 163-168

[35] Brunauer S, Emmett P H and Teller E. On a theory of the van der Waals adsorption of gases. J. Am. Chem. Soc, 1938, 60, 309

[36] Groen J C, Peffer L A A, Ramirez J P. Pore size determination in modified micro and mesoporous materials. Pitfalls and limitations in gas adsorption data analysis. Microporous and Mesoporous Materials, 2003, 60, 1-17

[37] Yang G W, Gao G Y, Wang C, et al. Controllable deposition of Ag nanoparticles on carbon nanotubes as a catalyst for hydrazine oxidation. Carbon, 2008 46, 747-752

[38] Patterson A L. The Scherrer Formula for X-Ray particle size determination. Phys. Rev, 1939, 56, 978-982

[39] Dresselhaus M S, Dresselhaus G, Saito R, et al. Raman spectroscopy of carbon nanotubes. Physics Reports, 2005, 409, 47-99

[40] Jorio A, Pimenta M A, Souza Filho A G, et al. Determination of nanotube properties by Raman spectroscopy. New J.Phys, 2003, 5, 139, 1-17.

[41] Cardenas J F, Gromov A. The effect of bundling on the G' band of single walled carbon nanotubes. Nanotechnology, 2009, 20

[42] Hu X, Wang T, Qu X, et al. In situ synthesis and characterisation of multiwalled carbon nanotube/Au nanoparticle composites. J. Phys. Chem. B, 2006, 110, 853-857

[43] Rance G A, Marsh D H , Nicholas R J, et al. UV-vis absorption spectroscopy of carbon nanotubes: Relationship between the π-electron plasmon and nanotube diameter. Chemical Physics Letters, 2010, 493, 19-23

[44] Yeh J M, Huang K Y, Lin S Y, et al. Noncovalent interaction between gold nanoparticles and multiwalled carbon nanotubes via an intermediatory. Journal of Nanotechnology, 2009, 217469

[45] Bokova S N, Obraztsova E D, Kukovecz A, et al. Raman study of diameter-dependent resonance effects and “metallic window” for different types of carbon nanotubes. Fullerenes, Nanotubes and Carbon Nanostructures, 2008, 16, 362-367.

[46] Itoh T, Uwada T, Asahi T, et al. Analysis of localised surface plasmon resonance by elastic light scattering spectroscopy of individual Au nanoparticles for surface enhanced Raman scattering. Canadian Journal of Analytical Sciences and Spectroscopy, 2007, 52 (3), 130-141.

[47] Su F Z, Liu Y M, Wang L C, et al. Ga-Al mixed oxide supported gold nanoparticles with enhanced activity for aerobic alcohol oxidation. Angew. Chem, 2008 120, 340-343

[48] US Environmental Protection Agency Twelve Principles of Green Chemistry. http://www.epa.gov/gcc/pubs/principles.html

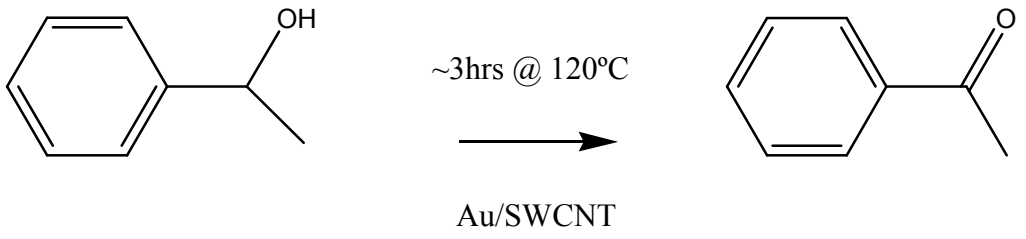

Scheme 1: Selective Oxidation of 1-Phenylethanol to Acetophenone

Figure 1A: N_2 adsorption-desorption isotherm of SWCNT

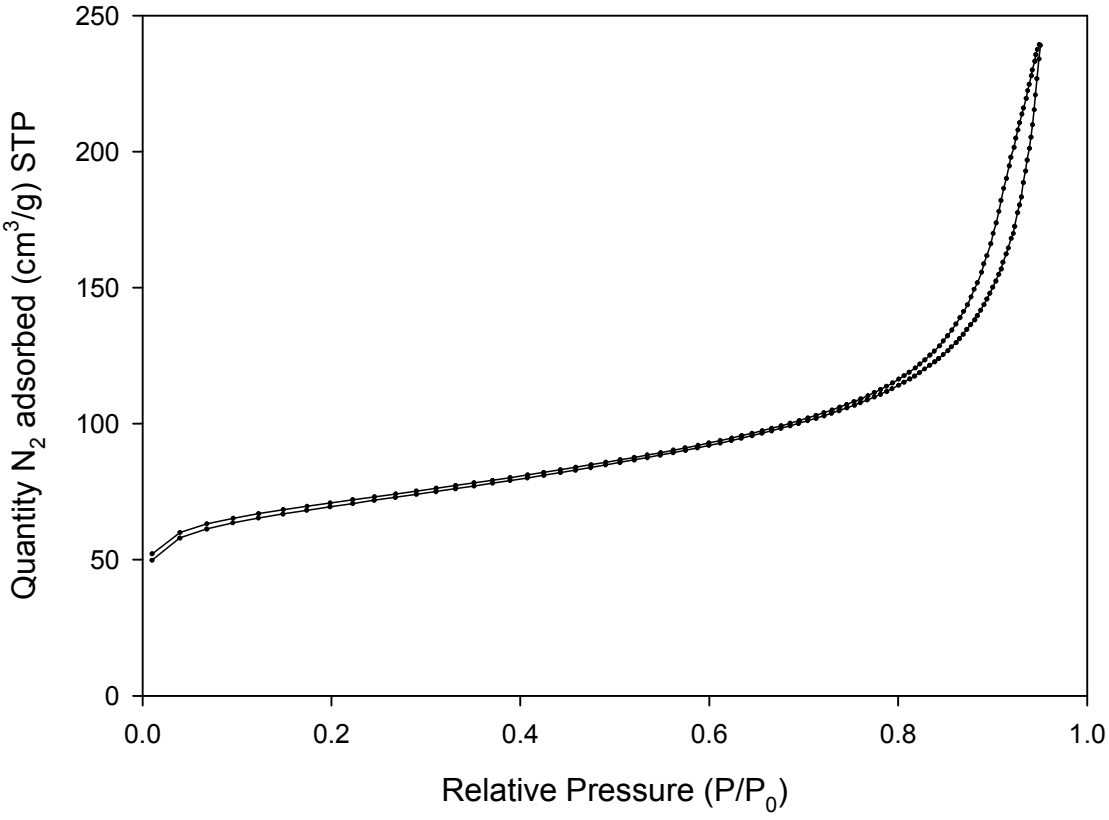

Figure 1B: N_2 adsorption-desorption isotherm of Au/SWCNT

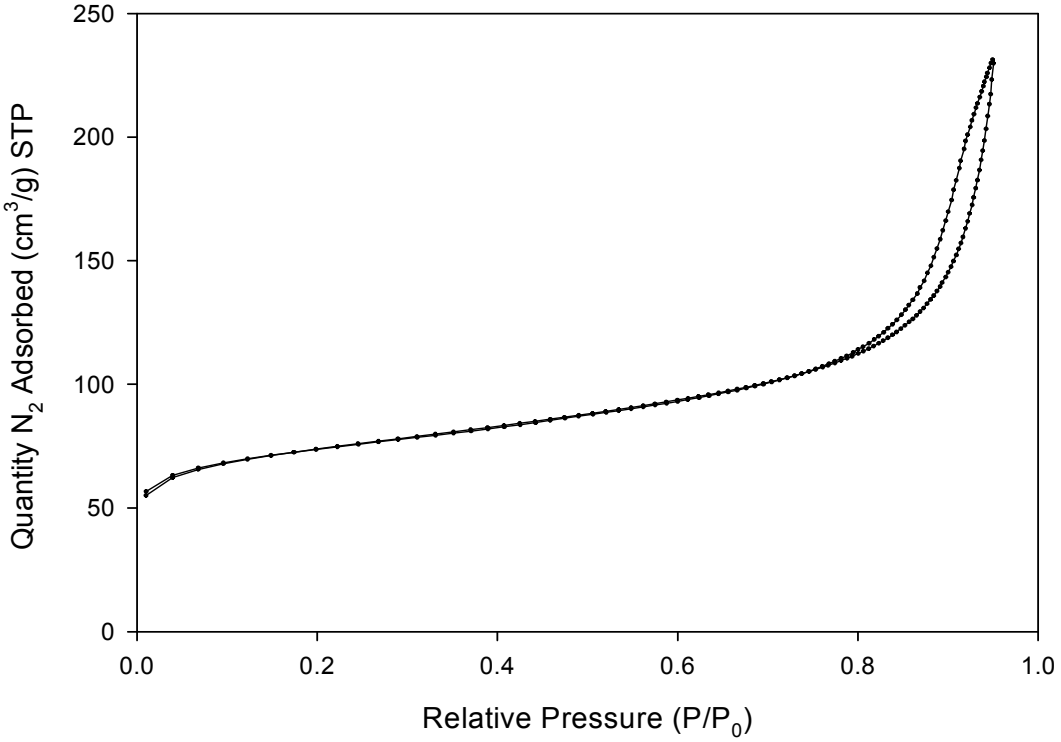

Figure 2: X-Ray Diffractograms of SWCNT (dotted) and Au/SWCNT (dashes)

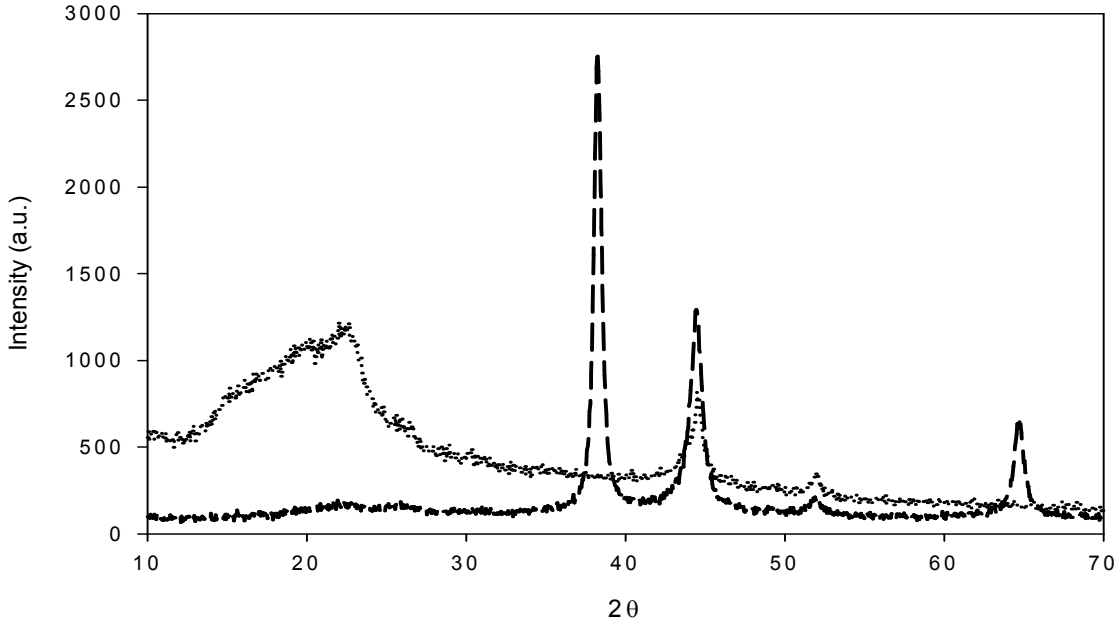

Figures 3: STEM images of 5% Au/SWCNT composite (A) 5% Au/SWCNT composite, (B) magnified version of (A) showing Au particles on the backbone of an SWCNT rope. Figure 3C shows a histogram of the Au particle size distribution for the Au/SWCNT composite.

A

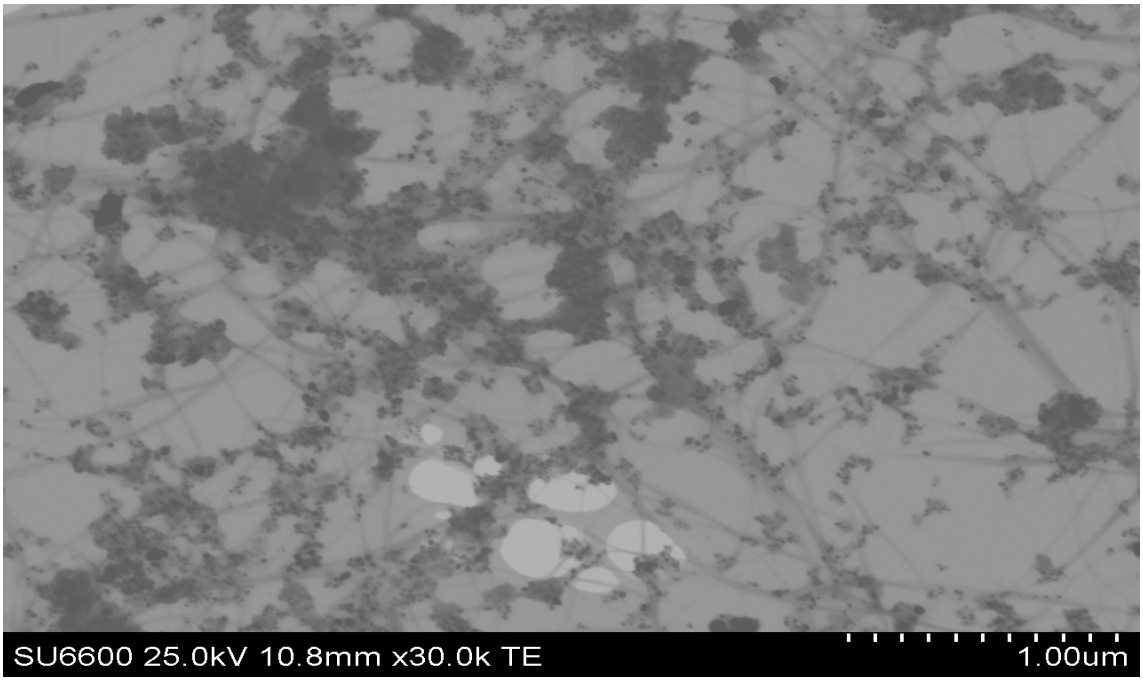

B

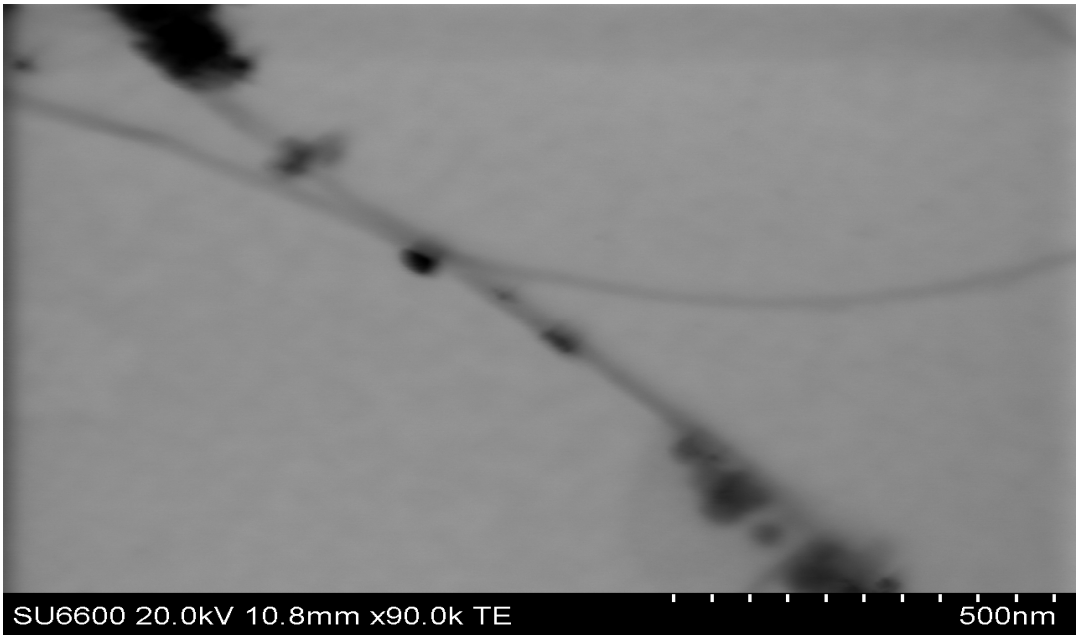
SU6600 20.0kV 10.8mm x90.0k TE
500nm

C

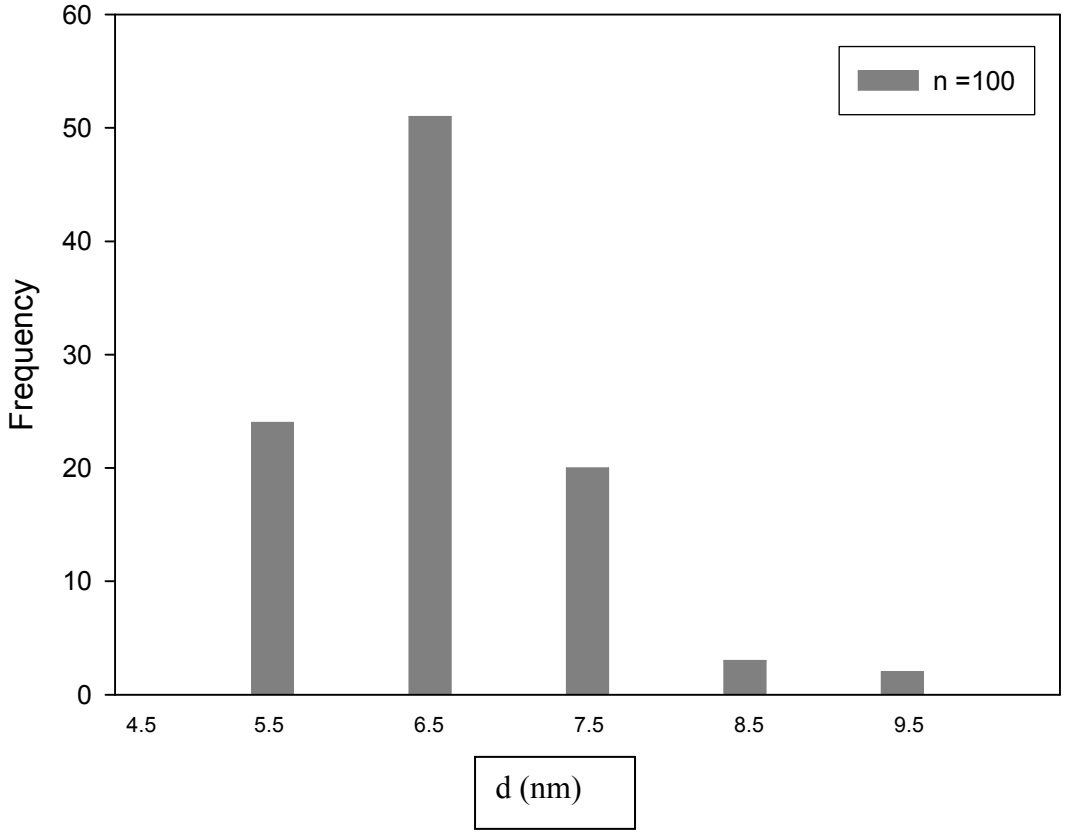
60
50
40
30
20
10
0
Frequency
n =100
4.5
5.5
6.5
7.5
8.5
9.5
d (nm)

Figures 4: Images of SWCNT (A), Au nanoparticles (B) and Au/SWCNT composite (C)

A

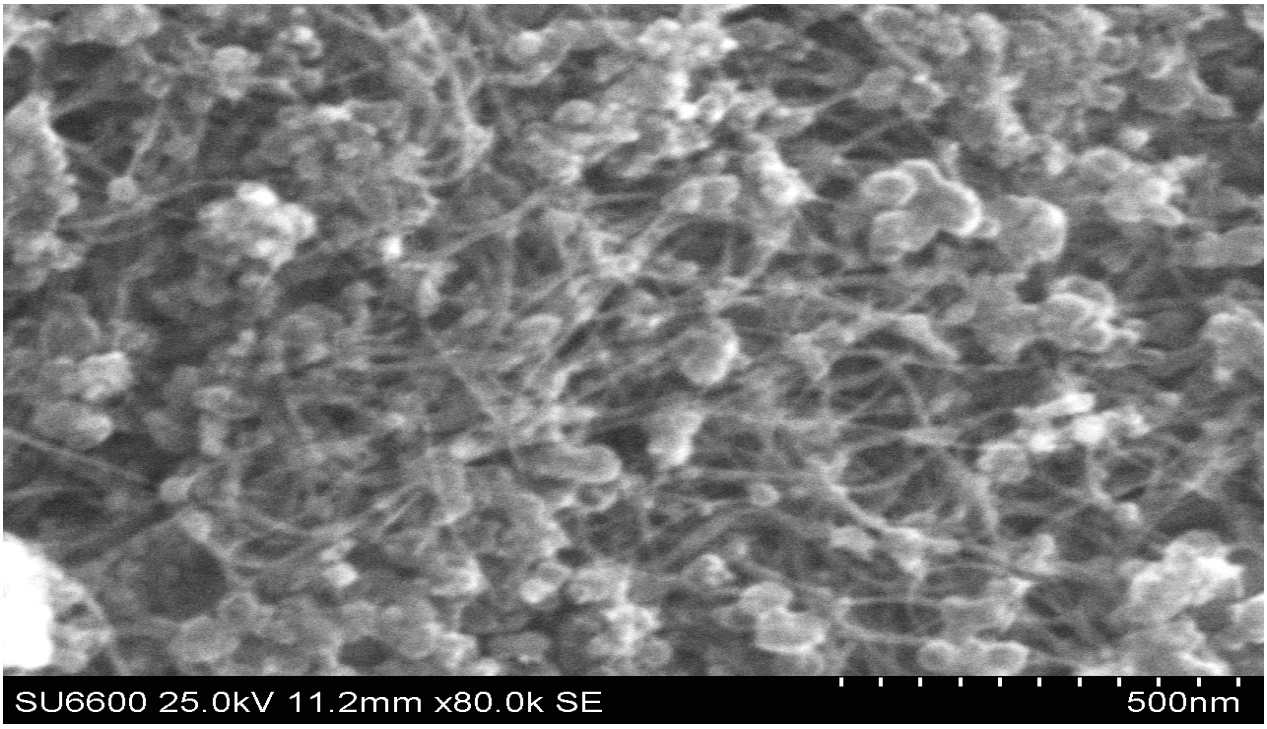

B

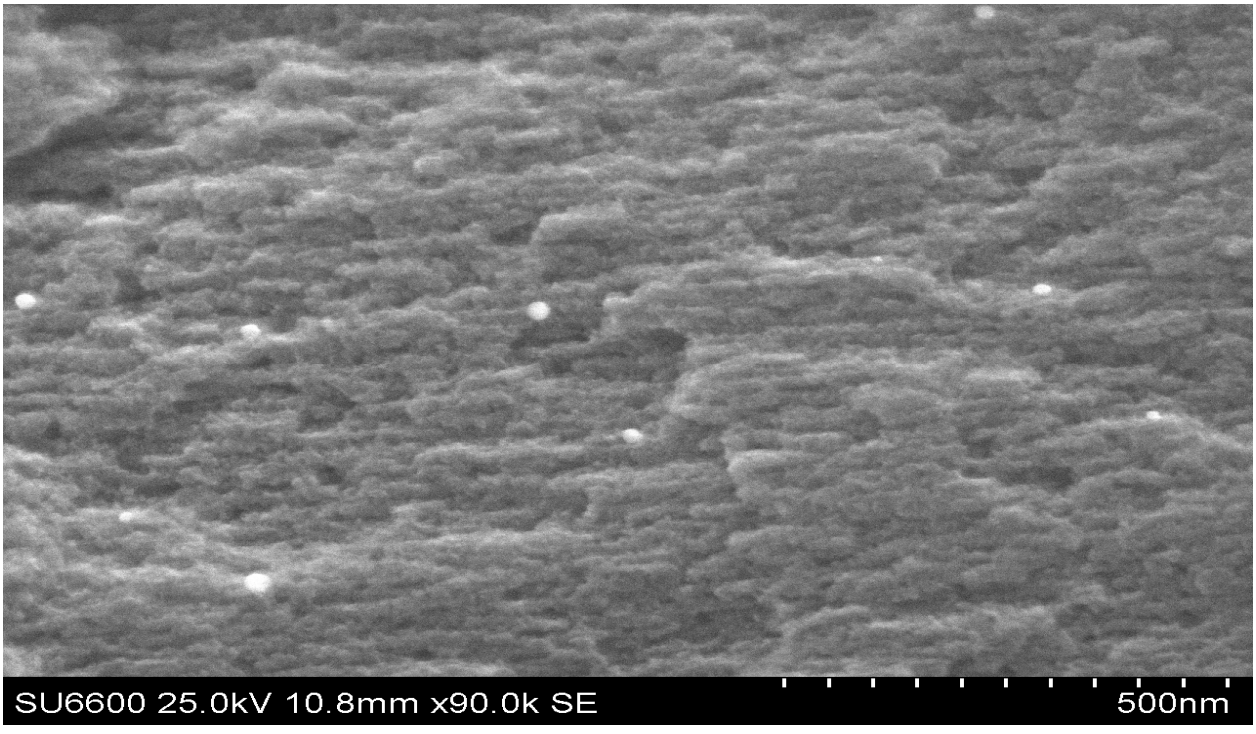

C

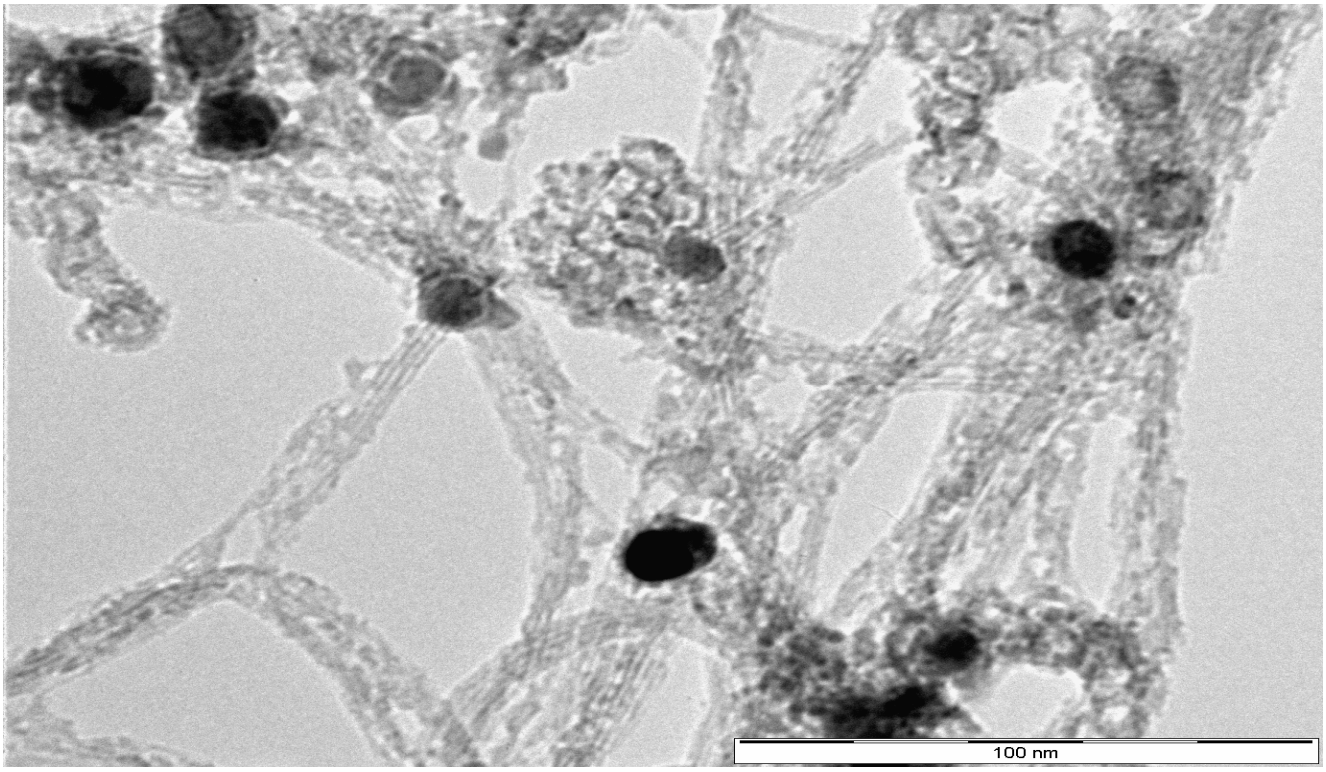

Figure 5: Raman Spectra of SWCNT (dotted) and 5%Au/SWCNT (full)

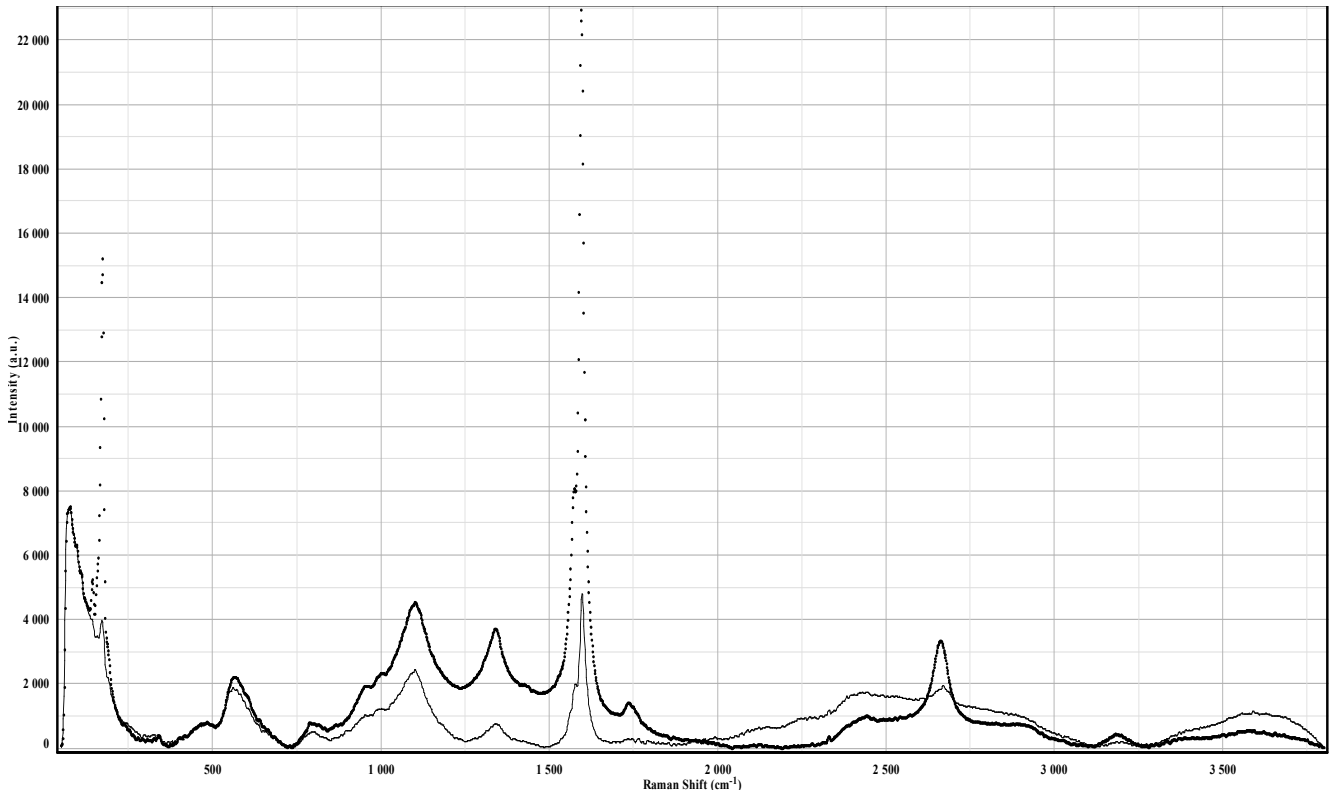

Figure 6: UV-Visible Spectra of SWCNT (dotted) and Au/SWCNT (dashes)

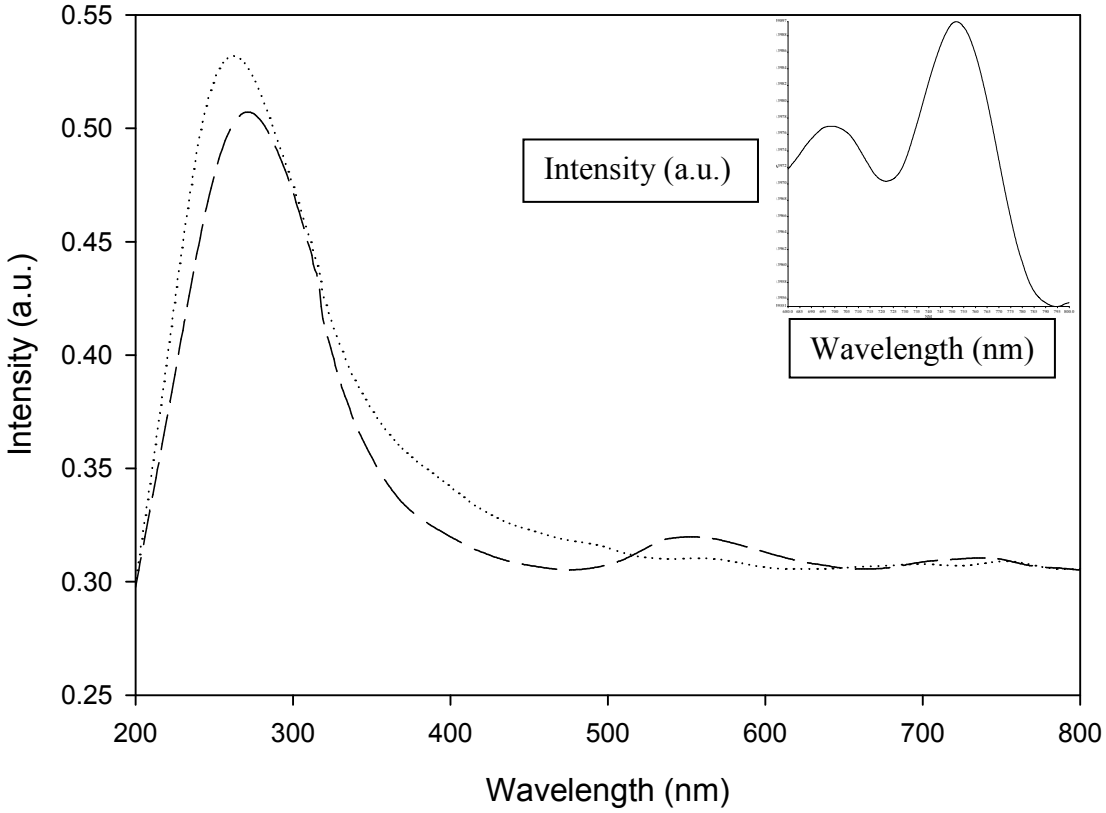

Figure 7: Plot of conversion v time for selective oxidation of 1-phenylethanol over 5% wt Au/SWCNT.